

1 **A model study of Abrahamsenbreen, a surging glacier in** 2 **northern Spitsbergen**

3

4 **J. Oerlemans¹, and W.J.J. van Pelt²**

5 [1]{ Institute for Marine and Atmospheric research Utrecht, Utrecht, The Netherlands }

6 [2]{Norsk Polar Institut, Tromsø, Norway }

7 Correspondence to: J. Oerlemans (j.oerlemans@uu.nl)

8

9 **Abstract**

10 The climate sensitivity of Abrahamsenbreen, a 20 km long surge-type glacier in northern
11 Spitsbergen, is studied with a simple glacier model. A scheme to describe the surges is
12 included, which makes it possible to account for the effect of surges on the total mass budget
13 of the glacier. A climate reconstruction back to 1300 AD, based on ice-core data from
14 Lomonosovfonna and climate records from Longyearbyen, is used to drive the model. The
15 model is calibrated by requesting that it produces the correct Little Ice Age maximum glacier
16 length and simulates the observed magnitude of the 1978-surge.

17 Abrahamsenbreen is strongly out of balance with the current climate. If climatic conditions
18 will remain as they were for the period 1989-2010, the glacier will ultimately shrink to a
19 length of about 4 km (but this will take hundreds of years). For a climate change scenario
20 involving a 2 m yr^{-1} rise of the equilibrium line from now onwards, we predict that in the year
21 2100 Abrahamsenbreen will be about 12 km long.

22 The main effect of a surge is to lower the mean surface elevation and thereby to increase the
23 ablation area, causing a negative perturbation of the mass budget. We found that the
24 occurrence of surges leads to a faster retreat of the glacier in a warming climate.

25 Because of the very small bed slope, Abrahamsenbreen is sensitive to small perturbations in
26 the equilibrium-line altitude. For a lowering of the equilibrium line by only 160 m, the glacier
27 would steadily grow into the Woodfjorddalen until after 2000 years it would reach the
28 Woodfjord and calving could slow down the advance.

29 The bed topography of Abrahamsenbreen is not known, and was therefore inferred from the
30 slope and length of the glacier. The value of the plasticity parameter needed to do this was

1 varied by +20 and -20 %. After recalibration the same climate change experiments were
2 performed, showing that in a warming climate a thinner glacier (higher bedrock in this case)
3 retreats somewhat faster.

4

5

6 **1 Introduction**

7 Abrahamsenbreen is a valley glacier in the northwestern part of Svalbard (79.10 N; 14.25 E),
8 originating at the icefield Holtedahlfonna (for more topographic information, see the
9 interactive map: <http://www.npolar.no/en/services/maps/>). It is about 20 km long and flows in
10 a northeasterly direction (Fig. 1). The glacier snout terminates on land and is only a few tens
11 of m a.s.l. The highest regions in the accumulation area are about 900 m a.s.l. (above mean
12 sea level). A large part of the accumulation area is rather flat with an altitude ranging between
13 600 and 750 m a.s.l. According to Hagen et al. (1993), the equilibrium-line altitude is around
14 600 m. The glacial river runs through the very flat Woodfjorddalen over a distance of about
15 15 km before it enters the Woodfjord.

16 The glacial history of northern Spitsbergen is only broadly known (Svendsen and Mangerud,
17 1997; Forman et al., 2004; Salvigsen et al., 2005). There is abundant evidence that the fjord
18 areas were deglaciated by 10 kyr BP (Before Present), and that during most of the Holocene
19 glaciers were less extensive than they are today. Abrahamsenbreen most likely reached its
20 maximum Holocene extent during the Little Ice Age, in line with the evidence for many large
21 glaciers in western and southern Spitsbergen (Hagen et al., 1993). One of the goals of this
22 paper is to see if this is in agreement with palaeoclimatic information derived from the
23 Lomonosovfonna ice cores (Pohjola et al., 2002; Divine et al., 2011) and the meteorological
24 record of Longyearbyen.

25 Abrahamsenbreen is a surging glacier. It is well known for its fine set of looped moraines
26 (Fig. 2) that were formed during and following the surge that took place around 1978 (Hagen
27 et al., 1993). The duration of the 1978 surge and the frequency with which surges occur is not
28 known. However, it is likely that the surge characteristics of Abrahamsenbreen are similar to
29 those of other gently sloping glaciers in Svalbard. These surges are of a less vigorous type
30 than observed on alpine glaciers like Variegated Glacier (Kamb et al., 1985), Medvezhiy
31 Glacier (Osipova and Tsvetkov, 1991) or North Gasherbrum Glacier (Mayer et al., 2011).
32 Surge characteristics of Svalbard glaciers vary considerably, but the common element is a
33 relatively long surging phase which lasts for several years (Dowdeswell et al., 1991; Melvold

1 and Hagen, 1998; Sund et al., 2009; Dunse et al., 2005). A ‘normal surge’ is an event in
2 which enhanced ice flow transports ice from higher regions to lower regions within a
3 relatively short time, in the end leading to a marked advance of the glacier front. However, in
4 a study of 50 glaciers, Sund et al. (2009) have also documented glacier surges in which the
5 enhanced motion stops before the stage of an advancing front is reached. The effect of the
6 surge then only implies a thinning of the accumulation region and a thickening of the ablation
7 region. In the case of Abrahamsenbreen there is no doubt that the 1978 surge was a full surge,
8 during which the glacier front advanced by at least 2 km.

9 After a surge, a glacier will be subject to a negative net surface mass balance, because the
10 mean surface elevation is lower than before the surge. However, because the ice flow
11 becomes (almost) stagnant, after some time the accumulation area will thicken. This implies
12 an increasing surface elevation, less melt in summer, and consequently the transition to a
13 stage in which the surface is steepening and the glacier volume is increasing until a new surge
14 is initiated. It is not a priori clear at which point in the cycle Abrahamsenbreen actually is.
15 According to the map of the equilibrium-line altitude over Svalbard provided in Hagen et al.
16 (1993), $E \approx 600$ m in the region of Abrahamsenbreen. For the parameterized glacier geometry
17 used in this study (discussed in section 3), this would imply that the glacier currently has a net
18 balance that is slightly negative. This is in agreement with the study of Nuth et al (2010), who
19 derived a net balance of -0.67 ± 0.14 m yr⁻¹ for the period 1966 – 2005. It should be noted that
20 the surge took place within this period.

21 There is no general concensus about the mechanism that causes glaciers in Svalbard to surge
22 (Murray et al., 2003). These glaciers flow over soft sediments, and the duration of surges is
23 significantly longer than for glaciers in steeper alpine terrain, which are at least partly hard-
24 bedded. Thermal regulation has been put forward as a likely mechanism, in which the switch
25 from frozen to warm bed conditions plays a central role (e.g. Fowler et al., 2003). However,
26 direct evidence for this theory does not exist. Oerlemans (2013) has suggested that the steady
27 accumulation of dissipative melt water in the accumulation zone plays an important role. In
28 recent years geometric changes caused by surging have been documented extensively (e.g.
29 Sund et al., 2009), but this has not yet resulted in a major step forward in our understanding.

30 Since so many glaciers on Svalbard are of the surging type, the question has arisen to what
31 extent surges interfere with the longer-term response of glaciers to climate change (Hagen et
32 al., 2005; Paasche, 2010). This question is of importance with respect to the climatic
33 interpretation of historical glacier fluctuations, and also needs to be considered when making

1 projections of glacier behaviour for scenarios of global warming. In the simple glacier model
2 used in this study surges are imposed and their effect on the mass budget is then implicitly
3 dealt with. By comparing model experiments with and without the surging mechanism the
4 potential role of surges in the evolution of Abrahamsenbreen is evaluated.

5 In this study the climate sensitivity of Abrahamsenbreen is studied with a simple glacier
6 model. A so-called *minimal glacier model* is used (Oerlemans, 2011), in which the ice
7 mechanics are strongly parameterized and the focus is on the total mass budget of the glacier.
8 In fact, the ice mechanics are reduced to a relation between the mean ice thickness, the glacier
9 length and the mean bed slope. The surge cycle is then imposed by making the proportionality
10 factor between length and thickness a prescribed function of time.

11 We are aware of the limitations of such a model. It does not give insight in why surges occur
12 and what determines the length of the surge cycle. However, since the mass budget of a (non-
13 calving) glacier is mainly determined by the mean surface elevation relative to the
14 equilibrium-line altitude, the details of the surface topography matter less. Therefore, useful
15 information about the climate sensitivity of a glacier can be obtained even without the
16 calculation of the spatially distributed fields of surface topography and ice velocity.

17 Hardly any measurements have been carried out on Abrahamsenbreen, making the modelling
18 of this glacier a real challenge.

19 The available data consists of (references to these data sources are given later in this paper):

- 20 • topographic maps for the years 1966 and 2002;
- 21 • aerial photographs from 1969 and 1990;
- 22 • a high-resolution satellite image (ASTER) acquired on 26 June 2001 ;
- 23 • mass balance observations on a nearby glacier (Kongsvegen, 25 km away);
- 24 • a map of the estimated equilibrium-line altitude over Svalbard;
- 25 • a map of annual precipitation over Svalbard;
- 26 • geomorphological information about the late Holocene history of Abrahamsenbreen.

27 In this paper we use these data to constrain and calibrate the model in the best possible way.
28 We consider this exercise to be useful, because for more than 99% of all glaciers in the world
29 no more information is available than maps, satellite images and photographs!

30

2 Modelling strategy and geometric input data

The geometry of the main stream of Abrahamsenbreen is simple with a very smooth surface profile along the flowline, indicating that the bed is also gently sloping. Major ramps or overdeepenings are likely absent, since they would certainly be reflected in features at the glacier surface (e.g. Raymond and Gudmundsson, 2005). Such a regular geometry is a prerequisite for the use of a minimal glacier model, which requires a small set of input parameters and can be calibrated easily with the limited data available. In a minimal glacier model the state variables are glacier length and mean ice thickness.

Before describing this model we will first summarize some of the information about the lower part of the glacier that is evident from the two aerial photographs (from 1969 and 1990), two topographic maps (1966 and 2002) and a satellite image (ASTER, 26 June 2001).

Terminal moraines from the tributary glaciers T4, T5, T9 and T10 (Fig. 1) are schematically mapped for three years (Fig. 3). The distance between the locations of the moraines in different years was calculated by projecting the moraine tips on the central flowline and measuring the displacement. For the displacement between 1990 and 1969 we found 4.5 and 4.7 km for M1 and M3 respectively, and 5.9 and 6.3 km for M2 and M4. Using the mean values of the paired moraines (left and right of the glacier), average corresponding ice velocities would be 219 m yr^{-1} for the lower region of the glacier, and about 290 m yr^{-1} for the middle part. The displacement between 2001 and 1990 is small, with corresponding velocities of 9 m yr^{-1} and 23 m yr^{-1} . If we think of the ice velocity as composed of a background part and a surge part, and we assume that the background part has been constant, it follows that the displacement of surface ice due to the surge would be 4.4 km for the lower part and 5.6 km for the middle part. It is not straightforward to convert these data into a total advance of the glacier front during the surge. Comparing the glacier outlines on the maps suggest a frontal advance of 1.8 km. However, the glacier front will have melted back from a more advanced position during the period 1978 (surge) to 2002 (map outline). Judging from the size of the moraine system (Fig. 2 & 3), retreat of the snout could have been at most 1.6 km during this period. This would imply that the total advance of the front related to the surge is not larger than 3.4 km.

Altitudinal profiles along the central flowline are shown in Fig. 4. The absolute error of the topographic maps in this area is not known, but the profiles appear to be consistent with the occurrence of the surge in 1978. The mean slope of the pre-surge profile (1966) is 0.035, that

1 of the post-surge profile (2002) 0.027. The mean difference in altitude ($\Delta\bar{h}$) between the
2 profiles is 51 m. It should be noted once more that by the year 2002 part of the glacier snout
3 has retreated. Hence, the mean difference in altitude shortly before and after the surge
4 probably was somewhat larger. The value of $\Delta\bar{h}$ cannot be taken directly as a measure of the
5 change in mean ice thickness ΔH_m , because the mean bed elevation is also different before
6 and after the surge (solely due to the change in glacier length). With the representation of the
7 bed chosen here (discussed shortly) we found $\Delta\bar{b} = 13$ m. Altogether, we used a value of
8 $\Delta H_m = 50$ m to characterize the change related to the surge.

9 Since the maps from which the profiles are taken are 36 years apart, the difference in mean
10 surface elevation can also partly be due to a non-zero surface balance rate during this period.
11 Unfortunately, in situ measurements are not available to check this. Nuth et al. (2010) infer a
12 negative mean balance rate for the period 1966 – 2005 from remote sensing data. However, in
13 their map of elevation changes over Northwest Spitsbergen (their Figure 5), the outlines for
14 Abrahamsenbreen are not identical to those inferred here from the 2002 topographic map. The
15 difference is mainly in the size of the accumulation area (larger in the present study), which
16 had a slightly positive balance rate during the period 1966 – 2005. In view of this, we have
17 not made any corrections to the value of $\Delta H_m = 50$ m as being characteristic for the surge.
18 We also note that with a significant different (smaller) value it is impossible to explain the
19 glacier advance during the surge in terms of mass conservation (which implies a direct
20 relation between change in glacier length and change in mean ice thickness).

21 The geometric set-up of the model is shown in Fig. 1. The main glacier is modelled as a
22 flowband with a constant width of 2000 m. It has its own surface mass budget, which is
23 definitely negative because it is almost entirely in the ablation zone. The main stream is fed by
24 tributary basins and glaciers, numbered T1,..., T10. The mass input from these tributaries is
25 parameterized in terms of a schematic geometry and depends on the climatic state. Details on
26 this are described in section 4. We assume that the tributaries have a considerably smaller
27 characteristic response time than the main glacier because they are steeper, implying that the
28 net balance of the tributaries is calculated as if they were in a quasi steady-state. This also
29 implies that tributaries having a negative net balance are simply ignored in the total mass
30 budget.

31 The bed topography is basically unknown. The surface of the glacier is smooth and has a
32 small slope (~ 0.03), and this suggests that a simple formulation of the bed profile is adequate.
33 A bed topography that can be handled well by the minimal glacier model reads

$$1 \quad b(x) = b_h \exp(-x/x_l) . \quad (1)$$

2 So the bed elevation drops off exponentially from a value b_h at the highest point of the
3 flowband ($x = 0$) to sea level for large values of x (see Fig. 1). The characteristic length scale
4 at which the bed becomes lower is denoted by x_l . We also considered to use a linear bed
5 profile, but this generates problems for glacier stands that are significantly larger than today
6 (bed far below sea level, which is unrealistic in this case). Here we chose $x_l = 12000$ m.
7 Admittedly, this value is not more than an educated guess based on the general picture of
8 valleys in northern Spitsbergen that are more deglaciated than the Abrahamsenbreen valley
9 (topographic map: <http://www.npolar.no/en/services/maps/>). The value for b_h is discussed
10 later.

11

12 **3 Glacier model**

13 The theory of minimum glacier models has been developed in Oerlemans (2011), and the
14 reader is referred to that work for details (freely available from the internet;
15 <http://www.staff.science.uu.nl/~oerle102/MM2011-all.pdf>). We only give a brief description
16 of the model version used here.

17 The starting point for the model formulation is the continuity equation:

$$18 \quad \frac{dV}{dt} = F + B_A + \sum_{i=1}^{10} B_i , \quad (2)$$

19 where V is the volume of Abrahamsenbreen, F (< 0) is the calving flux, B_A is the total
20 surface mass budget of Abrahamsenbreen, and the last term represents the mass input from
21 the tributary glaciers as defined in Fig. 1. The glacier length L is measured along the central
22 line on the glacier (Fig. 1). Since here we do not consider states of Abrahamsenbreen where
23 it calves into the Woodfjord, we set $F = 0$.

24 Because the glacier width w is assumed to be constant, the rate of change of ice volume can
25 be written as

$$26 \quad \frac{dV}{dt} = w \frac{d}{dt} (H_m L) = w \left(H_m \frac{dL}{dt} + L \frac{dH_m}{dt} \right) = B_{tot} , \quad (3)$$

27 where B_{tot} is the right-hand side of eq. (1), the total mass budget of the glacier.

28 The mean ice thickness is parameterized as (Oerlemans, 2011):

$$1 \quad H_m = S \frac{\alpha_m}{1 + \nu \bar{s}} L^{1/2}, \quad (4)$$

2 where \bar{s} is the mean slope of the bed over the glacier length and α_m and ν are constants. A
 3 ‘surge function’ S has been introduced, which makes it possible to impose a surge cycle. S is
 4 prescribed as a function of time. A rapid decrease of S mimics the surge, whereas a steady
 5 increase of S represents the quiescent phase during which the glacier thickness steadily
 6 increases. The precise form of $S(t)$ will be discussed later.

7 The parameterization of the mean ice thickness as described by eq. (4) gives a good fit to
 8 results from numerical flowline models. For $\bar{s} \rightarrow 0$ the mean thickness varies with the square
 9 root of the glacier length, which is in agreement with the perfectly plastic and Vialov
 10 solutions for a glacier/ice cap on a flat bed (Weertman, 1961; Vialov, 1958). The minimal
 11 glacier model was used earlier in a study of Hansbreen, southern Spitsbergen (Oerlemans et
 12 al., 2011). The bed topography of Hansbreen is known, and it was found that Eq. (4) matches
 13 the observed mean thickness for $\nu = 10$ and $\alpha_m = 3 \text{ m}^{1/2}$. However, Hansbreen is a non-
 14 surging tidewater glacier in a different geographical and geological setting, and among the
 15 very few glaciers with bedrock data we have therefore selected Kongsvegen as a better glacier
 16 to estimate the parameter α_m . Like Abrahamsenbreen, Kongsvegen is a surging glacier, which
 17 is currently in its quiescent phase (Melvold and Hagen, 1998). It is located not far away from
 18 Abrahamsenbreen (about 25 km). From the bed and surface profiles of Kongsvegen a value of
 19 $\alpha_m = 2.27 \text{ m}^{1/2}$ is found, indicating that here basal conditions allow for a lower resistance
 20 than in the case of Hansbreen. We have used the value of $\alpha_m = 2.27 \text{ m}^{1/2}$ as the best possible
 21 estimate for Abrahamsenbreen. However, different values of this parameter will be used later
 22 in a sensitivity test.

23 Using the chain rule for differentiation, the time rate of change of ice thickness can be
 24 expressed as

$$25 \quad L \frac{dH_m}{dt} = \frac{\alpha_m}{2(1 + \nu \bar{s})} S L^{1/2} \frac{dL}{dt} - \frac{\alpha_m \nu}{(1 + \nu \bar{s})^2} S L^{3/2} \frac{\partial \bar{s}}{\partial L} \frac{dL}{dt} + \frac{\alpha_m}{(1 + \nu \bar{s})} L^{3/2} \frac{dS}{dt}. \quad (5)$$

26 Combining with Eq. (3) then yields:

$$27 \quad B_{tot} = w \left(\frac{3\alpha_m}{2(1 + \nu \bar{s})} S L^{1/2} \frac{dL}{dt} - \frac{\alpha_m \nu}{(1 + \nu \bar{s})^2} S L^{3/2} \frac{\partial \bar{s}}{\partial L} \frac{dL}{dt} + \frac{\alpha_m}{(1 + \nu \bar{s})} L^{3/2} \frac{dS}{dt} \right). \quad (6)$$

28 Here B_{tot} is the total mass budget, i.e. the right-hand side of Eq. (3).

1 The prognostic equation for the length of the glacier can thus be written as:

$$2 \quad \frac{dL}{dt} = \frac{B_{tot}}{w(a+b)} - \frac{c}{(a+b)} \frac{dS}{dt}, \quad (7)$$

3 where

$$4 \quad a = \frac{3}{2} H_m; \quad b = -\frac{\nu H_m L}{(1+\nu\bar{s})} \frac{\partial\bar{s}}{\partial L}; \quad c = -\frac{H_m L}{S}. \quad (8)$$

5 From Eq. (7) it is clear that a sufficiently rapid decrease of S ($dS/dt \ll 0$) leads to a strong
6 increase in L (but not in V).

7 For the exponentially decaying bed profile described by Eq. (1) the mean bed slope over the
8 glacier length is easily found to be:

$$9 \quad \bar{s} = \frac{b_h(1 - e^{-L/x_l})}{L}. \quad (9)$$

10 The term $\partial\bar{s}/\partial L$, needed in the coefficient b in Eq. (8) is

$$11 \quad \frac{\partial\bar{s}}{\partial L} = -\frac{b_0(1 - e^{-L/x_l})}{L^2} + \frac{b_0 x_l^{-1} e^{-L/x_l}}{L}. \quad (9)$$

12 This concludes the formulation of the glacier model. When B_{tot} is known, Eq. (7) can be
13 integrated in time with a simple forward time-stepping scheme. The calculation of B_{tot} is
14 described in the next section.

15

16

17 **4 Formulation of the mass budget**

18 **4.1 Mass budget of the main glacier**

19 Mass balance measurements have been carried on a number of glaciers in Svalbard, but not on
20 Abrahamsenbreen. Glaciers with a mass-balance record of at least 10 years, as filed at the
21 World Glacier Monitoring Service, are Midtre Lovénbreen, Kongsvegen, Hansbreen and
22 Austre Brøggerbreen. Long-term mean balance profiles are shown in Fig. 5. These profiles
23 suggest that a schematic representation of the balance rate can be taken as a linear function of
24 altitude, i.e.

$$25 \quad \dot{b} = \beta(h - E), \quad (10)$$

1 where β is the balance gradient and E is the equilibrium-line altitude. Linear regression on the
 2 profiles shown in Fig. 5 yields values of β ranging from 0.0039 to 0.0053 m w.e. m^{-1} . The
 3 mean value is 0.0045 m w.e. m^{-1} , which is used in this study. It is clear from the available
 4 observations that a higher-order formulation, e.g. with a quadratic term in h , is not
 5 meaningful. However, according to Hagen et al. (1993; their Fig. 8), annual precipitation
 6 decreases significantly when going in northeasterly direction from the Holtedahlfonna,
 7 implying an increase in the equilibrium-line altitude of about 100 to 150 m over the length of
 8 Abrahamsenbreen (assuming a sensitivity of E with respect to changes in precipitation of -
 9 2.25 m per %, see section 6.1). This is taken into account by making E a function of x :

$$10 \quad E = E_0 + \gamma x, \quad (11)$$

11 where γ is the spatial gradient of the equilibrium-line altitude along the flowline of the glacier.
 12 From the glacier length and change of E we estimate $\gamma = 0.005$.

13 The total mass gain or loss can now be found by integrating the balance rate over the glacier
 14 surface:

$$15 \quad B_s = \beta \int_0^L \{H(x) + b(x) - E_0 - \gamma x\} dx = \beta(H_m + \bar{b} - E_0)L - \frac{\beta\gamma}{2}L^2, \quad (12)$$

16 where \bar{b} is the mean bed elevation of the glacier. For the exponentially decaying bed profile
 17 it is given by

$$18 \quad \bar{b} = \frac{b_h}{L} \int_0^L e^{-x/x_l} dx = \frac{x_l b_h}{L} (1 - e^{-L/x_l}). \quad (13)$$

19

20 **4.2 Tributary glaciers**

21 For the tributary glaciers feeding the main stream, some further analysis is required to arrive
 22 at useful estimates of the mass input. Although the tributary glaciers could be modelled in a
 23 similar way as the main glacier, we take a somewhat simpler approach in which the surface
 24 geometry is fixed. This is justified because the tributary glaciers have much larger mean
 25 slopes and therefore a weaker altitude - mass balance feedback.

1 We assume that a tributary glacier can be described as a basin with a length L_y and a width
 2 $w(y) = w_0 + qy$. Here y is a local coordinate running from the lowest part of the basin ($y = 0$)
 3 to the highest part of the basin ($y = L_y$). The surface elevation is taken as $h(y) = h_0 + sy$,
 4 where s is the surface slope. The parameters q and s are constants which are different for the
 5 individual basins. The total mass budget B_i of basin i is then obtained from

$$6 \quad B_i = \int_0^{L_y} \beta(b_0 + sy - E)(w_0 + qy) dy . \quad (14)$$

7 Evaluating the integral yields:

$$8 \quad B_i = \beta \left[w_0(b_0 - E)L_y + \frac{1}{2} \{ s w_0 + (b_0 - E)q \} L_y^2 + \frac{1}{3} s q L_y^3 \right] . \quad (15)$$

9 The geometric characteristics of the basins have been estimated from the topographic map
 10 and are summarized in Table I. All basins have a trapezoidal shape, some becoming narrower
 11 when going up ($q < 0$), some wider ($q > 0$). Due to the spatial gradient in E , see eq. (11), the
 12 basins which are located further downstream along the x-axis will experience a slightly higher
 13 equilibrium-line altitude. This is accounted for by applying a basin-dependent correction
 14 (Table I).

15

16 **5 Basic experiments**

17 For $S = 1$ and $E = 587$ m the model produces a steady-state glacier with a length of 17.5 km,
 18 which is close to the pre-surge length (we cannot define this precisely). A good match
 19 between the calculated and observed (pre-surge) mean surface elevation is obtained with
 20 $b_h = 323$ m, $\alpha_m = 2.27 \text{ m}^{1/2}$. The mean ice thickness then is 263 m. We refer to this state as
 21 the reference state. The corresponding mass inputs from the tributary basins are given in the
 22 last column of Table I. The net balance of the main glacier stream is -0.66 m w.e., and this is
 23 then compensated exactly by the mass input from the tributaries. Glaciers are never in steady
 24 state, and certainly not surging glaciers. Nevertheless, it is useful to have a steady state as a
 25 reference state, because it reveals basic properties of the glacier model. At this point it should
 26 be noted that the value of the bed parameter b_h is determined by the value of α_m . Although we
 27 believe that the value of α_m as discussed in section 3 is a good choice, we will later discuss a
 28 few sensitivity tests to show how the value of α_m affects the results.

1 The next step is to introduce the surge behaviour. The surge function is formulated as

$$2 \quad S(t) = C - S_a(t - t_0)e^{-(t-t_0)/t_s} + S_q(t - t_0) . \quad (16)$$

3 The surge starts at $t = t_0$ and the surge amplitude S_a determines by how much the thickness of
4 the glacier is reduced. The characteristic time scale of the surge is denoted by t_s . The last
5 term in eq. (16) represents the quiescent phase of the surge cycle, during which the glacier
6 steadily thickens because the mass flux is smaller than the balance flux. The constant C
7 should be chosen in such a way that the long-term mean value of $S(t)$ is close to one.

8 We use $t_s = 2.5$ yr. This value is based on the observation that most surges of Svalbard
9 glaciers typically last a few years (Sund et al., 2009). The value of S_q is determined by two
10 factors: the rate of mass addition in the accumulation area, and the degree to which the glacier
11 motion slows down after the surge. For the present case we have chosen values of S_a and S_q in
12 such a way that (i) the frontal advance related to the surge is reproduced, and (ii) the
13 difference in the mean ice thickness before and after the surge is in agreement with the
14 observations (about 50 m; section 2). We thus found $S_a = 0.168 \text{ yr}^{-1}$ and $S_q = 0.002 \text{ yr}^{-1}$.

15 The duration of the surge cycle for Abrahamsenbreen is not known. For most glaciers the
16 duration of the quiescent phase is in the 50 to 500 yr range (e.g. Dowdewell et al., 1991).
17 Because Abrahamsenbreen is a large and rather flat glacier in a relatively dry climate, we
18 have chosen a surge cycle of $\Theta = 125$ yr. Later we will show sensitivity tests that reveal how
19 the particular choice of Θ affects the results.

20 A model simulation in which the surge mechanism is switched on at some point in time (after
21 the glacier has reached the reference state defined above) is shown in Fig. 6. As discussed
22 above, a surge leads to a sudden decrease of the mean ice thickness and associated negative
23 net balance (-0.3 m yr^{-1} just after the surge). During the quiescent phase the net balance
24 gradually becomes positive and the ice thickness increases, but this is not enough to
25 compensate for the mass loss during and just after the surge. Therefore the glacier length
26 decreases until a new equilibrium is reached after about 1000 years. The net effect of the
27 surging mechanism thus is to reduce the long-term glacier length. This is in agreement with
28 earlier studies (Adalgeirsdóttir et al., 2005; Oerlemans, 2011).

29

30 **6 Response of Abrahamsenbreen to climate change**

31 **6.1 Reference simulation**

1 In this section we describe how a reference simulation, including the surging behaviour, has
2 been obtained. A simulation of the evolution of Abrahamsenbreen during the late Holocene
3 requires a plausible climatic forcing. In the present model climate change is imposed by
4 adjusting the equilibrium-line altitude according to

$$5 \quad E(t) = E_0 + E'(t) . \quad (17)$$

6 The annual perturbation of the equilibrium-line altitude is denoted by $E'(t)$, and determined
7 by annual temperature and precipitation anomalies, denoted by T' (in K) and P' (in %),
8 respectively. $E'(t)$ is thus written as

$$9 \quad E'(t) = \frac{\partial E}{\partial T} T'(t) + \frac{\partial E}{\partial P} P'(t) , \quad (18)$$

10 where the sensitivities $\partial E / \partial T$ and $\partial E / \partial P$ are assumed to be constant. Sensitivities have been
11 determined for Nordenskiöldbreen with a detailed energy and mass balance model (Van Pelt
12 et al. 2012; Table 2), and here we use their values:

$$13 \quad \frac{\partial E}{\partial T} = 35 \text{ m K}^{-1}; \quad \frac{\partial E}{\partial P} = -2.25 \text{ m \%}^{-1} . \quad (19)$$

14 For many glaciers in a more Alpine setting values of $\partial E / \partial T$ are of the order of 100 m K^{-1}
15 (e.g. Oerlemans, 2001). The value for $\partial E / \partial T$ given in eq. (19) thus appears as rather small.
16 This is due to the fact that in the high Arctic summer temperature anomalies, which mainly
17 determine the sensitivity, are much smaller than annual temperature anomalies. This has been
18 taken into account in the determination of the sensitivities.

19 The input data to calculate E' are taken from Van Pelt et al. (2013). In this paper a climate
20 reconstruction back to 1300 AD was made on the basis of ice-core data from
21 Lomonosovfonna as well as climate records from Longyearbyen. For details the reader is
22 referred to Divine et al. (2011) and Van Pelt et al. (2013). The temperature and precipitation
23 anomalies, relative to the period 1989-2010, are shown in Fig. 7, and the corresponding
24 history of the equilibrium-line altitude in Fig. 8. The most prominent feature in the
25 reconstructed temperature record is the Little Ice Age (LIA), lasting from the late 16th century
26 until the end of the 19th century, with long-term temperatures typically 4 K below the
27 medieval and present-day levels. The reconstruction does not reveal a clear correlation
28 between temperature and precipitation anomalies. The variation of the equilibrium-line
29 altitude is substantial. During the period 1750 – 1850, the equilibrium line was about 200 m
30 lower than in medieval times.

1 The value of E_0 is optimized in such a way that the simulated maximum glacier length in
2 1978 corresponds with the observed length. This yields $E_0 = 657$ m. Note that E' is defined
3 with respect to the period 1989-2010, implying that its mean value over the period 1300-2010
4 is not zero. In the climate reconstruction used here, the value of E during the period 1989-
5 2010 was 76 m larger than the long-term mean since 1300 AD.

6 The simulated glacier length (Fig. 8) appears to be in good agreement with geological
7 evidence (distribution of moraines, strandlines and floodplains). There is general agreement
8 that Abrahamsenbreen reached a Holocene maximum extent during the LIA, like most
9 glaciers in northern Spitsbergen (e.g. Forman et al., 2004; Salvigsen and Høgvard, 2005;
10 Humlum et al., 2005). According to our model, Abrahamsenbreen would have had a length of
11 about 5 km in medieval times, and started to grow in the 16th century until it reached LIA size
12 (between 18 and 22 km) in the second half of the 19th century. For the calculation shown in
13 Fig. 8, for the period after 2010 the value of E has been kept constant to the 1989–2010 value.
14 This clearly implies steady retreat, but the time-scale at which this happens is large. This is an
15 implication of the very small bed slope and the related strong altitude – mass balance
16 feedback (Oerlemans, 2011).

17 Fig. 9 shows the mass inputs (in m^3 of ice per year) of the tributary basins and glaciers
18 corresponding to the simulation shown in Fig. 8. Although the inputs are highly correlated,
19 there are large differences in the absolute changes of mass input through time. The input from
20 tributary glaciers T4, T5 and T10 is sometimes zero. For T9 this happens just a few times.
21 The other basins always deliver some mass to the main glacier, but the amounts can halve or
22 double during high or low values of E' .

23 We refer to the simulation just described as the reference simulation. The model has been
24 tuned in the best possible way given the limited amount of observations. There appears to be
25 no evident discrepancy between the simulated glacier evolution and the geological evidence.

26

27 **6.2 The effect of surging**

28 The question of how surges interfere with the long-term response of glaciers to climate
29 change has been raised several times (Hagen et al., 2005; Paasche, 2010). Although the
30 present model does not initiate surges by means of an internal mechanism, it does include the
31 main effect of a surge on the surface mass budget of a glacier related to the reduction of the
32 mean surface elevation. Since a lower surface elevation implies a more negative mass budget,

1 one would expect that a regularly surging glacier would have a smaller long-term mean
2 glacier length.

3 With the present model set-up it is not possible to just switch off the surging mechanism,
4 because by virtue of eq. (16) the model glacier would be in the quiescent phase continuously
5 and the ice thickness would increase for ever. However, a meaningful way to study the effect
6 of surging is to vary the duration of the surge cycle and see how this effects the long-term
7 mean glacier length. To make a fair comparison between runs with different surge cycles, the
8 constant C in eq. (16) is adjusted in such a way that the mean value of $S(t)$ is equal to one over
9 the integration period.

10 Fig. 10 shows a comparison of runs with a longer (doubled, i.e. 250 yr) and shorter (halved,
11 i.e. 62.5 yr) surge cycle. The integrations have been extended until 3000 AD, with the
12 equilibrium-line altitude equal to the mean value over the period 1989 – 2010. This leads to a
13 steady decay of the glacier, implying that the current size of Abrahamsenbreen is far too large
14 for the climatic conditions that prevailed during the past few decades.

15 The effect of a different surge frequency is small until 1900 AD, but much more obvious
16 afterwards. This is related to the fact that, with a glacier in a state of decay, the mass-balance
17 effect of surges works in the same direction as the climatic forcing. Moreover, the extension
18 of the glacier surface is into a region with anomalous high ablation rates. In contrast, for a
19 growing glacier, the mass-balance effect of surges works against the climatic imbalance and is
20 therefore less visible.

21 Many more numerical experiments were carried out with different surge parameters. An
22 increased surge amplitude (larger value of S_a) enhances the effect on the long-term glacier
23 length because it implies a larger drop of the mean surface elevation. When the surge takes
24 longer (larger value of t_s) there is a similar effect.

25 The decay of the glacier after the year 2000 is a remarkable feature, given the relatively small
26 climatic forcing. In the model simulation, after 1989 the equilibrium line is 76 m higher than
27 for the period 1300 -1989. The new steady state length is about 4 km, but it takes 500 years to
28 approach this state.

29 The extreme climate sensitivity of Abrahamsenbreen is a consequence of the small bed slope.
30 Basic theory on the relation between E and L for a schematic glacier geometry (constant
31 glacier width) shows that a first-order estimate of the sensitivity is given by (Oerlemans,
32 2001, 2012):

$$\frac{\partial L}{\partial E} = -\frac{2}{\bar{s}} \quad (20)$$

where \bar{s} is the mean bed slope. For the bed parameters used here, a typical value of \bar{s} is 0.015, implying that $\partial L/\partial E \approx -133$. So a 50 m change in the equilibrium-line altitude would imply a change in glacier length of 6.7 km! Oerlemans (2011) also reveals that the sensitivity as defined by eq. (20) is larger when the accumulation zone is wider than the ablation zone. For Abrahamsenbreen this implies that the value of 133 probably is a conservative estimate.

6.3 Sensitivity to bed elevation

The basic unknown parameters that can be adjusted to make the model produce the correct glacier length and mean surface elevation are the bed elevation parameter b_h , the shape parameter α_m , and the reference equilibrium-line altitude E_0 . We thus have three parameters and two constraints, implying that a unique set of parameters cannot be found. In section 5 the problem was solved by assuming that the value of α_m is the same as for Kongsvegen. Although Kongsvegen is also in a post-surge state and is located in a similar geological setting, it is still possible that the value of α_m for Abrahamsenbreen differs significantly. Therefore some calculations were carried out with perturbed values of α_m , namely +20 % and -20 %.

Changing the value of α_m implies that a recalibration has to be done by adjusting the values of b_h and E_0 to get the correct glacier length in 1978 and the correct mean surface elevation. For a 20 % larger value of α_m ($2.72 \text{ m}^{1/2}$) we found $b_h = 241 \text{ m}$ (instead of 323 m) and $E_0 = 643 \text{ m}$ (instead of 657 m). For a 20 % smaller value of α_m ($1.82 \text{ m}^{1/2}$) we found $b_h = 412 \text{ m}$ and $E_0 = 670 \text{ m}$. Because the ice thickness is proportional to α_m , it is not surprising that the adjustments in b_h are quite significant. However, the required changes in the value of E_0 are rather small.

The evolution of the glacier length for the three different tunings is shown in Fig. 11. It is interesting to see that for the case with $\alpha_m = 1.82 \text{ m}^{1/2}$ the surge in 1853 produces a slightly longer glacier than in 1978. The differences among the three cases are small for the period of glacier growth, and significant for the period of glacier retreat after 2000. This is a consequence of the fact that during the period of glacier growth the glacier length was rather close to its equilibrium value most of the time (because, irrespective of short-term

1 fluctuations, the equilibrium line drops gradually). After the year 2000, the glacier is strongly
2 out of balance for the imposed forcing, and the effect of different ice thicknesses on the rate
3 of retreat turns out to be more pronounced.

4 In summary, we conclude that the simulated glacier evolution depends on the choice of α_m ,
5 but not in a dramatic way. The characteristic behaviour of Abrahamsenbreen for the imposed
6 forcing is rather similar for the three different tunings.

7 8 **6.4 Sensitivity to changes in the equilibrium-line altitude**

9 By means of numerical modelling it has been shown that a glacier on an isolated mountain
10 bordered by a flat plane will grow to infinity if the equilibrium line is lowered beyond a
11 certain critical value (Oerlemans, 1981; Fig. 10). This occurs because the feedback of the
12 mean surface elevation on the balance rate keeps the total mass budget positive. In the present
13 model the bed profile decays exponentially to a constant value (namely, sea level), and the
14 critical value of the equilibrium-line altitude described above is very likely to be in the
15 system. In the case of Abrahamsenbreen this would imply that for a certain drop of the
16 equilibrium line the glacier would grow and grow until the front reaches the Woodfjord and
17 only mass loss by calving could stabilize the glacier at some point.

18 Critical (bifurcation) points in a dynamical system normally imply an increasing sensitivity
19 and response time when the critical point is approached. Theoretically, when approaching the
20 critical point the sensitivity and response time go to infinity. The large response time
21 suggested by Fig. 10 actually suggests that Abrahamsenbreen may indeed be close to the
22 critical point. With these considerations in mind we have carried out a set of integrations with
23 different values of E' after 2010 AD.

24 Fig. 12 shows glacier length for different climatic perturbations, all started with the calibrated
25 glacier history until 2010 AD. Clearly, for $E' = -160$ m the glacier quickly comes in a state of
26 runaway growth, and it ultimately grows out of the model domain. For $E' = -120$ m the
27 glacier approaches a steady state, but very slowly. For further increasing values of E' , steady
28 states are approached more quickly. In fact, the curves in Fig. 12 show that the response time
29 decreases when the steady-state glacier length is smaller. This is not a direct consequence of
30 the glacier size, but related to the corresponding increase in the mean bed slope and the larger
31 distance (in parameter space) to the critical point.

1 **6.4 The future of Abrahamsenbreen**

2 It is very likely that the Arctic will be subject to further warming, which will have a large
3 impact on the glaciers of Svalbard. Reduced sea ice may lead to higher precipitation rates, but
4 it is questionable whether this could stop the retreat of the glaciers. According to eq. (19), a
5 precipitation increase of about 15% per degree warming would be required to keep the
6 equilibrium line in place. A detailed analysis of the precipitation regime in the Arctic with a
7 comprehensive climate model suggests a sensitivity of 4.5% increase per degree of
8 temperature warming (Bintanja and Selten, 2004). Although this is significantly more than the
9 global value of 1.6 to 1.9 % increase per degree, it is by no means sufficient to prevent the
10 rise of the equilibrium line when temperatures go up.

11 The future evolution of Abrahamsenbreen can be studied with the present model, because it
12 has been calibrated and no further assumptions are needed to define an initial state.
13 Nevertheless, one should be aware of the schematic nature of the model and the limited data
14 available for Abrahamsenbreen, implying that the constraints are not very tight. The results
15 given below should therefore be considered as indicative of what is a possible scenario rather
16 than a prediction.

17 We have carried out a set of integrations until 2150 AD, with an equilibrium line that rises
18 linearly in time, according to

$$19 \quad E'(t) = \mu_E(t - 2010) . \quad (20)$$

20 Again, the anomaly is defined with respect to the period 1989-2010; time t is in years AD.
21 With the aid of eq. (19) changes in equilibrium-line altitude can be related to changes in
22 temperature and precipitation. For instance, $\mu_E = 1 \text{ m yr}^{-1}$ would correspond to a warming
23 rate of 0.028 K yr^{-1} , or to a warming rate of 0.04 K yr^{-1} combined with an increase in
24 precipitation of 0.016 \% yr^{-1} . In all the integrations the surge period and amplitude have been
25 kept constant.

26 Fig. 13 shows the result for $\mu_E = 1 \text{ m yr}^{-1}$, which we consider as a typical value for the
27 expected warming in the Arctic. In this case the length of Abrahamsenbreen is predicted to be
28 reduced to 12.7 km by the year 2100. The corresponding reduction in volume is 66 % of the
29 value in 2010. The net balance rate for the entire system and the input from the tributaries is
30 also shown. By the year 2100 the input from the tributary glaciers has been reduced to
31 virtually zero, because they have a negative net balance.

1 Future glacier length projections for different values of μ_E are compared in Fig. 14. It can be
2 seen that glacier retreat is steadily accelerating although the forcing changes linearly in time.
3 This is due to the height – mass balance feedback: the glacier gets more and more out of
4 balance and the surface becomes subject to higher ablation rates.

5

6 **7 Discussion**

7 In this paper we have applied a simple model to study the climate sensitivity of
8 Abrahamsenbreen. We have demonstrated that even with a limited amount of information a
9 meaningful calibration can be carried out, and some conclusions can be drawn about the
10 present state of balance and the future of Abrahamsenbreen under conditions of climate
11 change.

12 Although the main trunk of Abrahamsenbreen has a relatively simple geometry, the total
13 glacier system is complicated with many basins and tributary glaciers providing mass to the
14 central flowband. The parameterization we have chosen to represent the geometry is effective
15 and contains sufficient information to quantify the overall mass budget. Admittedly, the
16 assumption that the tributaries are in a quasi steady-state is perhaps not always satisfied when
17 the climatic forcing changes rapidly. However, modelling a glacier system like
18 Abrahamsenbreen with a two-dimensional (vertically-integrated) or three-dimensional ice-
19 flow model, and dealing explicitly with the tributaries would be a complicated task requiring
20 a large amount of input data. We therefore believe that the method used here is suitable to
21 study the dynamics of complex glacier systems with many tributaries.

22 We found that the effect of surges on the long-term size of the glacier is significant, but not
23 dramatic. Since surges are imposed rather than internally generated, only the impact of surges
24 on the mass budget, by lowering of the mean surface elevation, could be dealt with. On the
25 basis of our calculations (Fig. 11), we expect that in a warming Arctic surging glaciers are
26 prone to retreat somewhat faster than non-surging glaciers. It is likely that the effect of
27 surging is larger for glaciers with a larger surge amplitude. However, when comparing the
28 surge amplitude of Abrahamsenbreen with that of some other glaciers in Svalbard (e.g.
29 Skobreen, Kongsvegen, Monacobreen, Nathorstbreen; Sund et al., 2009), it appears that
30 Abrahamsenbreen is quite typical. We therefore think that our results apply to other surging
31 glaciers as well.

32

1 It is encouraging that forcing the model with an independently derived climate history leads to
2 a glacier evolution that is in line with the geological and geomorphological evidence. This
3 certainly lends credibility to the approach, and makes projections for the future more
4 believable. If the present climatic conditions would persist, we predict that Abrahamsenbreen
5 will shrink considerably (to a length of about 4 km). In the case of future warming of a few
6 degree K, the glacier will ultimately disappear, but this will take a few hundred years. Due to
7 the fact that Abrahamsenbreen flows into a valley with a very small bed slope, its sensitivity
8 to climate change is very large. Our calculations suggest that Abrahamsenbreen is rather close
9 to a critical point, marking the onset of a runaway situation in which the glacier will grow into
10 Woodfjorden for only a modest drop of the equilibrium line (160 m). However, this would
11 take a long time (a few thousand years, Fig. 12).

12 The large sensitivity of Abrahamsenbreen is probably not an exception. Many large glaciers
13 on Spitsbergen have small slopes and are subject to similar processes. An earlier modelling
14 study of Hansbreen in south-Spitsbergen also revealed a large sensitivity to climate change
15 (Oerlemans et al., 2011). The consequence of these findings is that a temperature increase of 1
16 to 2 K would remove most of the ice from Spitsbergen, although it may take a long time
17 (hundreds to thousands of years). This is in line with the growing evidence for an only
18 marginally glaciated landscape in Spitsbergen during the Holocene Climatic Optimum (e.g.
19 Humlum et al., 2005).

20

21 **References**

22 Aðalgeirsdóttir G., H. Björnsson, F. Pálsson and E. Magnússon (2005). Analysis of a surging
23 outlet glacier of Vatnajökull ice cap, Iceland. *Annals of Glaciology* **42**, 23-28.

24 Bintanja R. & Selten F.M. 2014. Future increases in Arctic precipitation linked to local
25 evaporation and sea-ice retreat. *Nature* **509**, 479-482. Doi: 10.1038/nature13259.

26

27 Divine D., Isaksson E., Martma T., Meijer H., Moore J., Pohjola V., van de Wal R. &
28 Godtlielsen F. 2011. Thousand years of winter surface air temperature variations in
29 Svalbard and northern Norway reconstructed from ice core data. *Polar Research* **30**, 7379,
30 doi:10.3402/polar.v30i0.7379.

31 Dowdeswell J.A., Hamilton G.S. & Hagen J.O. 1991. The duration of the active phase on
32 surge-type glaciers: contrasts between Svalbard and other regions. *Journal of Glaciology*
33 **37**, 388-400.

34 Dunse T., Schuler T.V., Hagen J.O. & Reijmer C.H. 2012: Seasonal speed-up of two outlet

- 1 glaciers of Austfonna, Svalbard, inferred from continuous GPS measurements. *The*
2 *Cryosphere* 6, 453-466, doi: 10.5194/tc-6-453-2012.
- 3 Forman S., Lubinsky D., Ingólfsson Ó., Zeeberg D., Snyder J.A. & Matishov G.G. 2004. A
4 review of postglacial emergence on Svalbard, Franz Josef Land and Novaya Zemlya,
5 northern Eurasia. *Quaternary Science Reviews* 22, 1391-1434.
- 6 Fowler A.C., Murray, T., and F.S.L. Ng 2001: Thermally controlled glacier surging. *J.*
7 *Glaciol.*, 42 (159), 527-538.
- 8 Hagen J.O., Liestøl O., Roland E. & Jørgensen T. 1993. *Glacier atlas of Svalbard and Jan*
9 *Mayen*. Norsk Polarinstitut Medd. nr. 129.
- 10 Hagen J.O., Eiken T., Kohler J. & Melvold, K. 2005. Geometry changes on Svalbard glaciers:
11 mass-balance or dynamic response? *Annals of Glaciology* 42, 255-261.
- 12 Humlum O., Elberling O., Hormes A., Fjordheim K., Hansen O.H. & Heinemeier J. 2005.
13 Late-Holocene glacier growth in Svalbard, documented by subglacial relict vegetation and
14 living soil microbes. *The Holocene* 15, 396-407, doi: 10.1191/0959683605hl817rp.
- 15 Kamb B., Raymond C.F., Harrison W.D., Engelhardt H.F., Echelmeyer K.A., Humphrey
16 N.F., Brugmann M.M. & Pfeffer T. 1985. Glacier surge mechanism, 1982-1983 surge of
17 Variegated Glacier, Alaska. *Science* 227, 469-479.
- 18 Mayer C., Fowler A.C., Lambrecht A. & Scharrer, K.: A surge of North Gasherbrum Glacier,
19 Karakorum, China. *J. Glaciol.* 57 (204), 904-916, 2011.
- 20 Melvold K. & Hagen J.O. 1998. Evolution of a surge-type glacier in its quiescent phase:
21 Kongsvegen, Spitsbergen, 1964-95. *Journal of Glaciology* 44 (147), 394-404.
- 22 Murray T., Strozzi T., Luckman A., Jiskoot H. & Christakos P. 2003. Is there a single surge
23 mechanism? Contrast in dynamics between glacier surges in Svalbard and other regions.
24 *Journal of Geophysical Research (Solid Earth)*, doi: 10.1029/2002JB001906.
- 25 Nuth C., Moholdt G., Kohler J., Hagen J.O. & Käab A. 2010. Svalbard glacier elevation
26 changes and contribution to sea level rise. *Journal of Geophysical Research* 115 (F01008),
27 doi: 10.1029/2008JF001223.
- 28 Oerlemans J. 1981. Some basic experiments with a vertically-integrated ice-sheet model.
29 *Tellus* 33, 1-11.
- 30 Oerlemans, J. 2011. *Minimal Glacier Models*. Second edition. Igitur, Utrecht University,
31 ISBN 978-90-6701-022-1.

- 1 Oerlemans J. 2012. Linear modeling of glacier fluctuations. *Geografiska Annaler* 94A, 183-
2 194, doi: 10.1111/j.1468-0459.2012.00469.x
- 3 Oerlemans J., Jania J. & Kolondra L. 2011. Application of a minimal glacier model to
4 Hansbreen, Svalbard. *The Cryosphere* 5, 1-11. Doi: 10.5194/tc-5-1-2011.
- 5 Osipova G.B. & Tsvetkov D.G. 1991. Kinematics of the surface of a surging glacier
6 (comparison of the Medvezhiy and Variegated Glacier. *IAHS Publ. no.208 (Glaciers-
7 Ocean-Atmosphere Interactions)*, 345-357.
- 8 Paasche Ø. 2010. *Reconstructing climate change: not all glaciers suitable*. *EOS Transactions*
9 *(AGU)* 91 (21), 189-190.
- 10 Pohjola V., Martma T., Meijer H., Moore J., Isaksson E., Vaikmae R. & Van De Wal R. 2002.
11 Reconstruction of three centuries of annual accumulation rates based on the record of
12 stable isotopes of water from Lomonosovfonna, Svalbard. *Annals of Glaciology* 35, 57–62.
- 13 Raymond M.J. & Gudmundsson G.H. 2005. On the relationship between surface and basal
14 properties in glaciers, ice sheets, and ice streams. *Journal of Geophysical Research* 110
15 (B8), doi: 10.1029/2005JB003681.
- 16 Salvigsen O. & Høgvard K. 2005. Glacial History, Holocene shoreline displacement and
17 palaeoclimate based on radiocarbon ages in the area of Bockfjorden, north-western
18 Spitsbergen, Svalbard. *Polar Research* 25(1), 15-24.
- 19 Svendsen J.I. & Mangerud J. 1997. Holocene glacial and climatic variations on Spitsbergen,
20 Svalbard. *The Holocene* 7, 45-57.
- 21 Sund M., Eiken T., Hagen J.O., and Kääb A. 2009. Svalbard surge dynamics derived from
22 geometric changes. *Annals of Glaciology* 50, 50-60.
- 23 Van Pelt W. J. J., Oerlemans J., Reijmer C.H., Pohjola V.A., Pettersson R. & van Angelen
24 J.H. 2012. Simulating melt, runoff and refreezing on Nordenskiöldbreen, Svalbard, using a
25 coupled snow and energy balance model. *The Cryosphere* 6, 641-659, doi:10.5194/tc-6-
26 641-2012.
- 27 Van Pelt W. J. J., Oerlemans J., Reijmer C.H., Pettersson R., Pohjola V.A. & Divine D. 2013.
28 An iterative inverse method to estimate basal topography and initialize ice flow models.
29 *The Cryosphere* 7, 987-1006, doi:10.5194/tc-7-987-2013.
- 30 Vialov S.S. 1958. Regularities of glacial shields movement and the theory of plastic viscous
31 flow. *International Association of Hydrological Sciences Publications* 47, 266–275.
- 32 Weertman J. 1961 Stability of ice-age ice sheets. *Journal of Geophysical Research* 66, 3783-
33 3792.

1

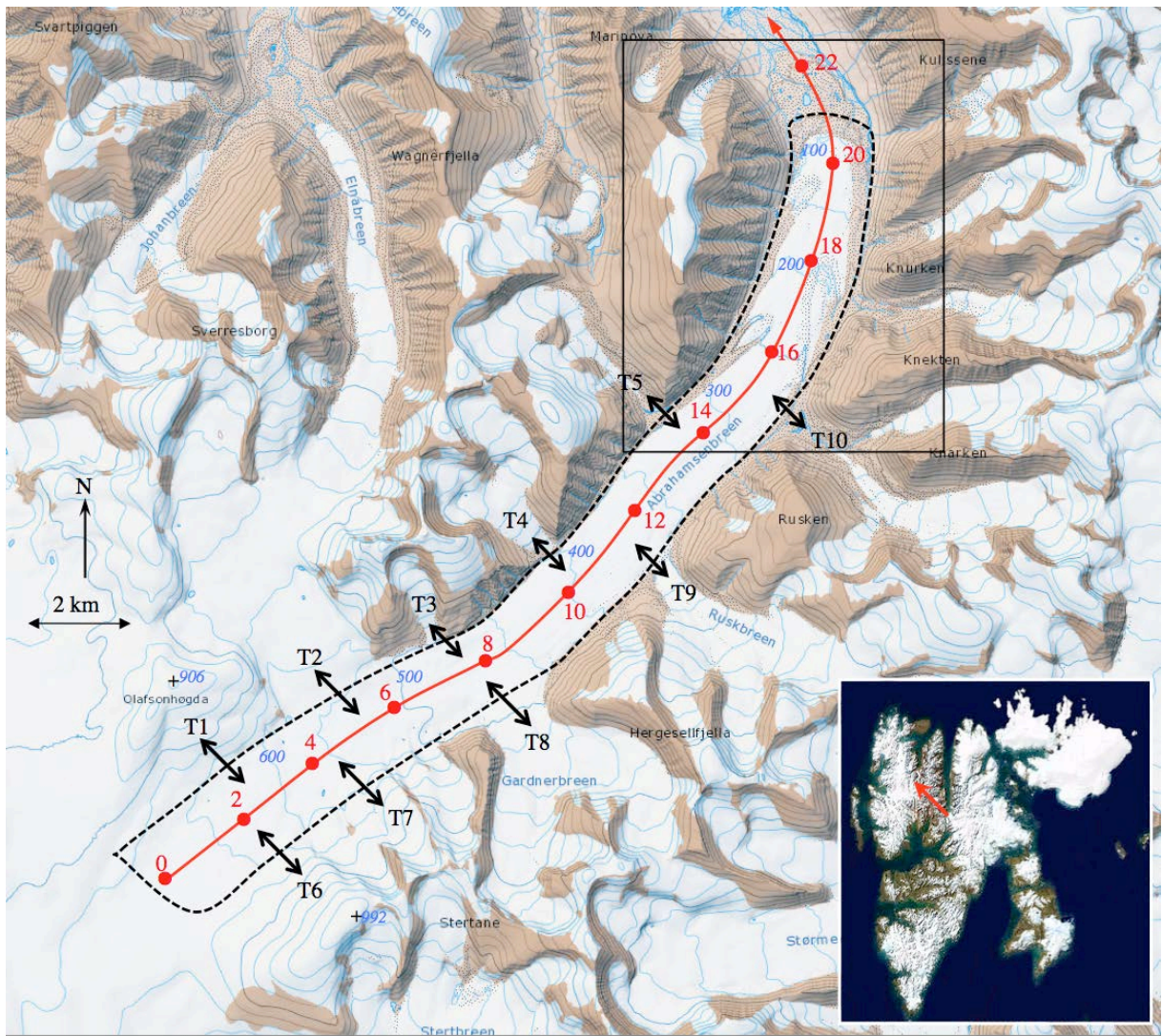
basin	L_y (m)	w_0 (m)	b_0 (m)	s	q (m)	$E_{b,corr}$ (m)	B_{ref} (m ³ yr ⁻¹)
T1	2100	4200	650	0.119	-1.00	0	8.4x10⁶
T2	4600	2600	550	0.058	0.0	15	4.9x10⁶
T3	2100	300	480	0.257	0.18	25	4.4x10⁵
T4	3400	400	410	0.163	0.71	44	3.9x10⁵
T5	4100	300	320	0.186	0.54	65	3.1x10⁵
T6	1800	2300	650	0.147	-0.65	0	4.1x10⁶
T7	2100	3500	600	0.120	-0.12	11	4.8x10⁶
T8	4200	1300	500	0.103	0.82	25	2.9x10⁶
T9	5800	600	430	0.090	0.70	55	8.6x10⁵
T10	5600	300	280	0.145	0.54	77	1.9x10⁵

2

3 **Table I.** Parameter values of the geometric characteristics of the basins that feed the main
4 stream. See Fig. 1 for the location of the basins. The last column shows the mass input (*ice*
5 volume) to the main glacier corresponding to the reference state described in the next section.

6

7



2

3

4 **Fig. 1.** Map of Abrahamsenbreen in northern Spitsbergen (inset), originating from the icefield
 5 Holvedahlfonna (lower left corner of the map). The red line shows the flow line along which
 6 the length is defined; numbers in red indicate distance from the glacier head in km. Basins
 7 and tributary glaciers delivering mass to the main stream are numbered T1 to T5 (left) and
 8 T6 to T5 (right). Isohypses on the glacier in m a.s.l. are shown in blue. Glacier stand in 1990, i.e.
 9 after the 1978 surge. Note that looped moraines are actually shown on the map. The rectangle
 10 in the upper part refers to the area covered by the aerial photograph of Figure 2. Courtesy:
 11 map: Norwegian Polar Institute; Landsat image: NASA.

12

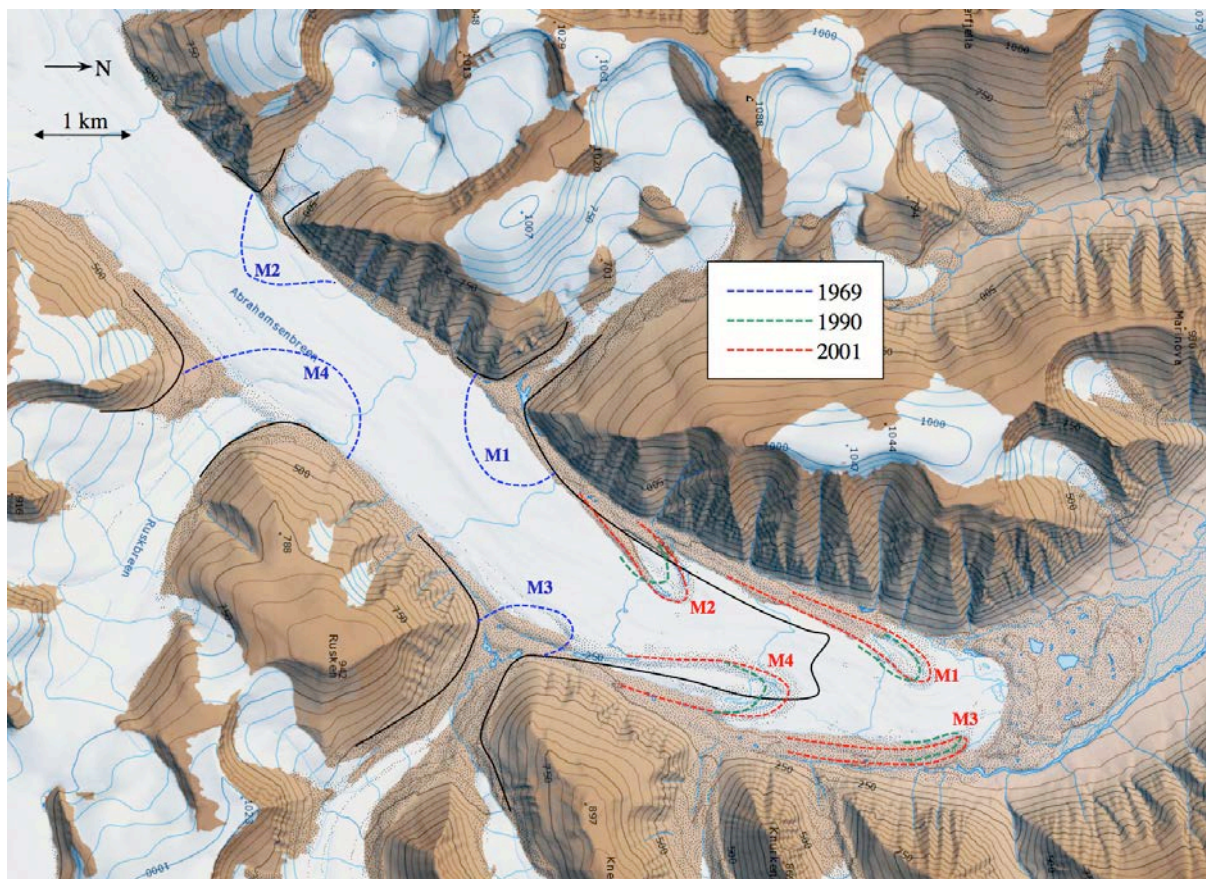
13

14



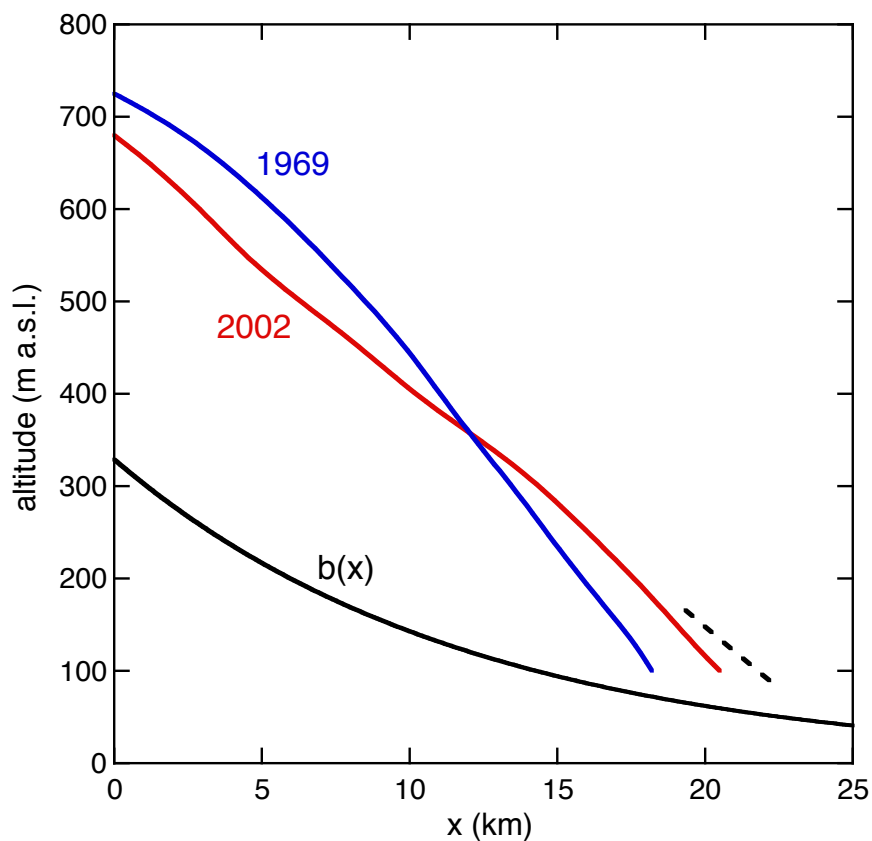
1
2
3
4
5
6
7
8

Fig. 2. Moraine loops on the lower part of Abrahamsenbreen, formed by rapid displacement of terminal moraines from tributary glaciers during the surge of 1978 (Aerial photograph S903134 1990; ©Norsk Polarinstitut)



1
2
3
4
5
6
7
8
9
10
11
12
13
14
15
16

Fig. 3. A close-up of the lower part of Abrahamsenbreen. The black solid lines indicate the glacier margin in 1966 (topographic map from the Norsk Polarinstitut). The moraine loops are numbered M1 to M4, and their migration has been visualized by using dashed lines of different colour to indicate the approximate positions in different years. The 1969 and 1990 locations have been taken from aerial photographs (S691493 and S903134; ©Norsk Polarinstitut), the 2001 locations from an ASTER-image (26 June 2001; NASA). Note that the map has been rotated over 90° with respect to Figs. 1 and 2.



1

2

3 **Fig. 4.** Altitude profiles along the central flowline of Abrahamsenbreen derived from
 4 topographic maps. The surge took place around 1978. The dashed line indicates a possible
 5 maximum extension of the glacier immediately after the surge. The reference bed profile is
 6 shown as $b(x)$.

7

8

9

10

11

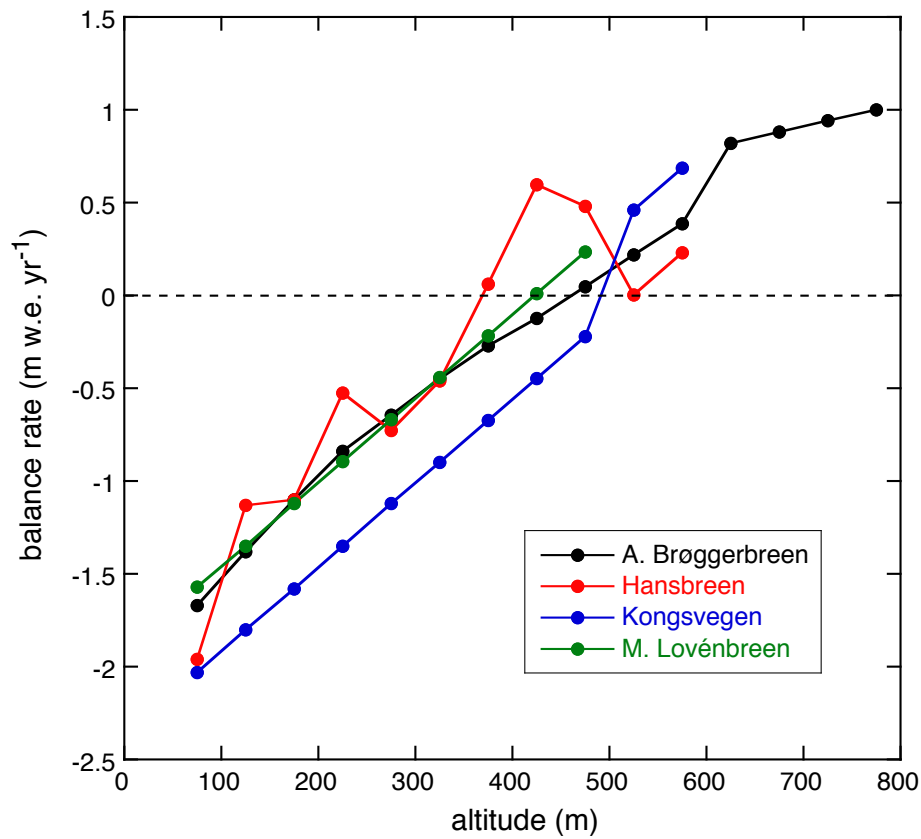
12

13

14

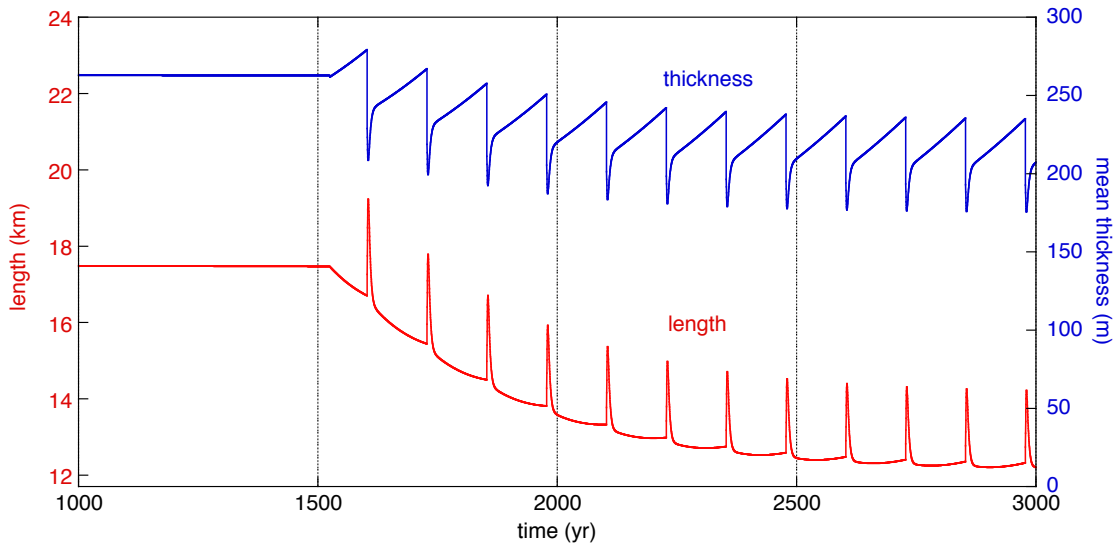
15

16



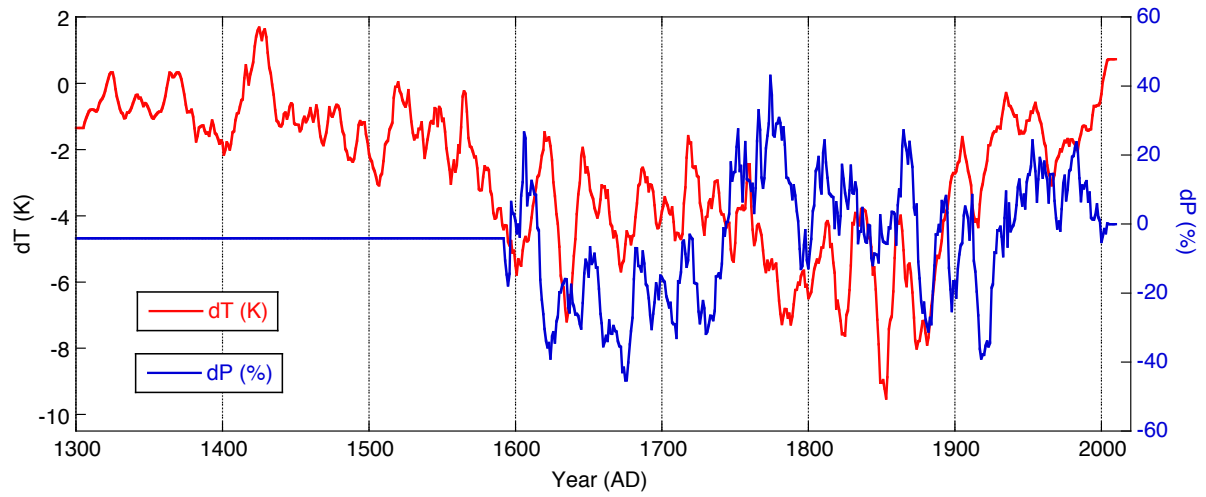
1
2
3
4
5
6
7
8
9
10
11
12
13
14
15
16

Fig. 5. Observed mean balance profiles for Austre Brøggerbreen (1990-2009), Hansbreen (1991-2009), Kongsvegen (2000-2009) and Midtre Løvenbreen (2000-2009). Data from the World Glacier Monitoring Service (Zürich).



- 1
- 2
- 3
- 4
- 5
- 6
- 7
- 8
- 9
- 10
- 11
- 12
- 13
- 14
- 15
- 16
- 17
- 18
- 19

Fig. 6. Surge event as imposed to the model by eq. (16).



1

2 **Fig. 7.** Climate history used to simulate the evolution of Abrahamsenbreen during the late
 3 Holocene (Van Pelt et al., 2013). Shown are anomalies of the annual mean temperature and
 4 the annual precipitation.

5

6

7

8

9

10

11

12

13

14

15

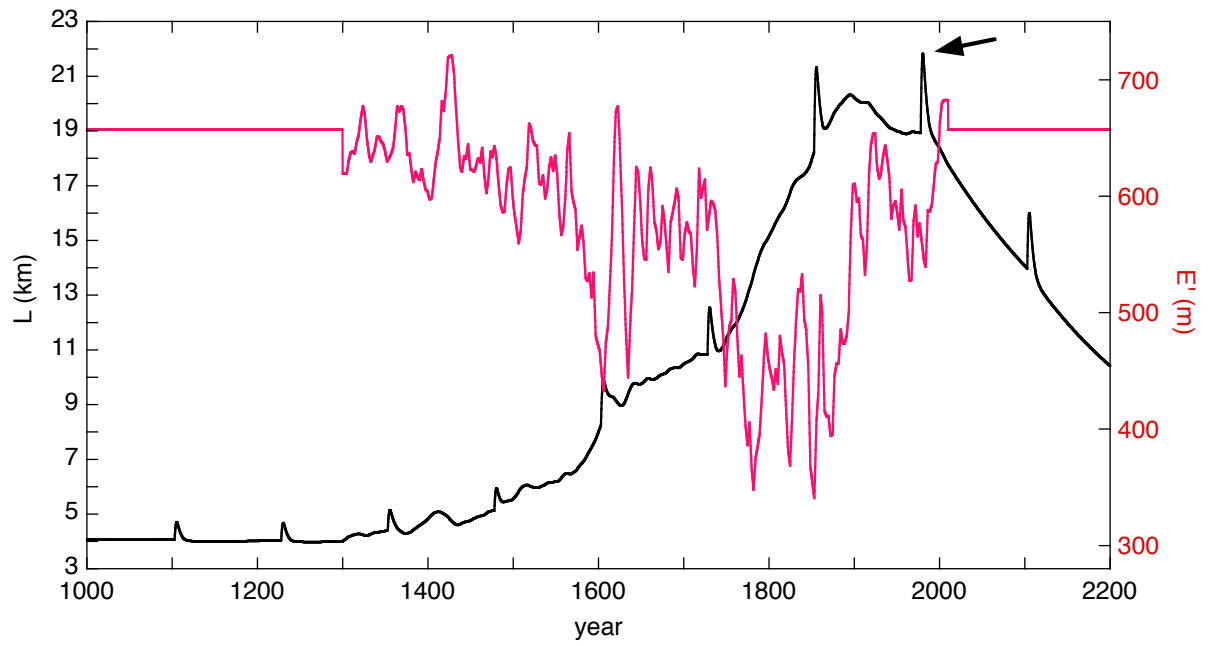
16

17

18

19

20



1

2 **Fig. 8.** Glacier length (in black, scale at left) and equilibrium-line altitude (in red, scale at
 3 right) from the simulation of Abrahamsenbreen. The arrow indicates the 1978 surge of the
 4 glacier.

5

6

7

8

9

10

11

12

13

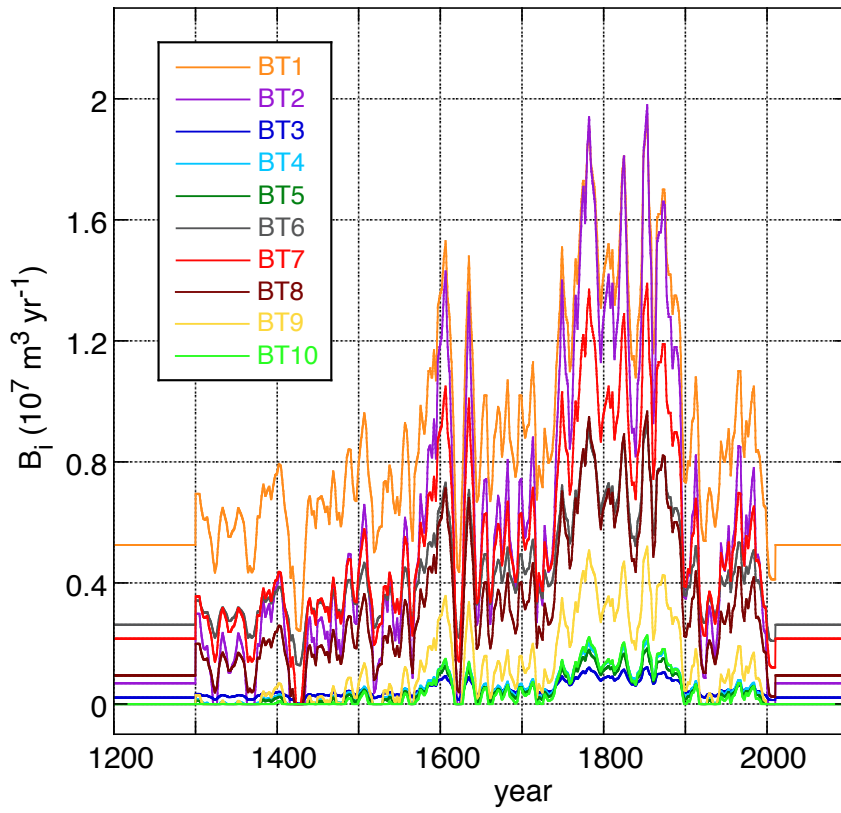
14

15

16

17

18



1

2 **Fig. 9.** Mass input from the ten tributary basins and glaciers for the simulation shown in Fig.
 3 8. The location of the basins is shown in Fig. 1.

4

5

6

7

8

9

10

11

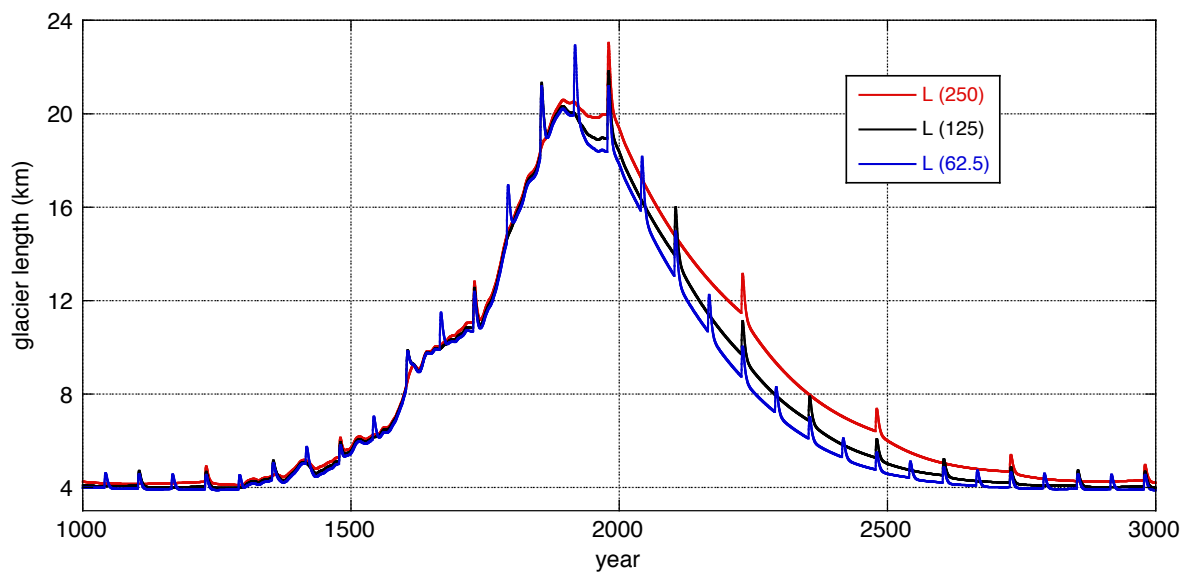
12

13

14

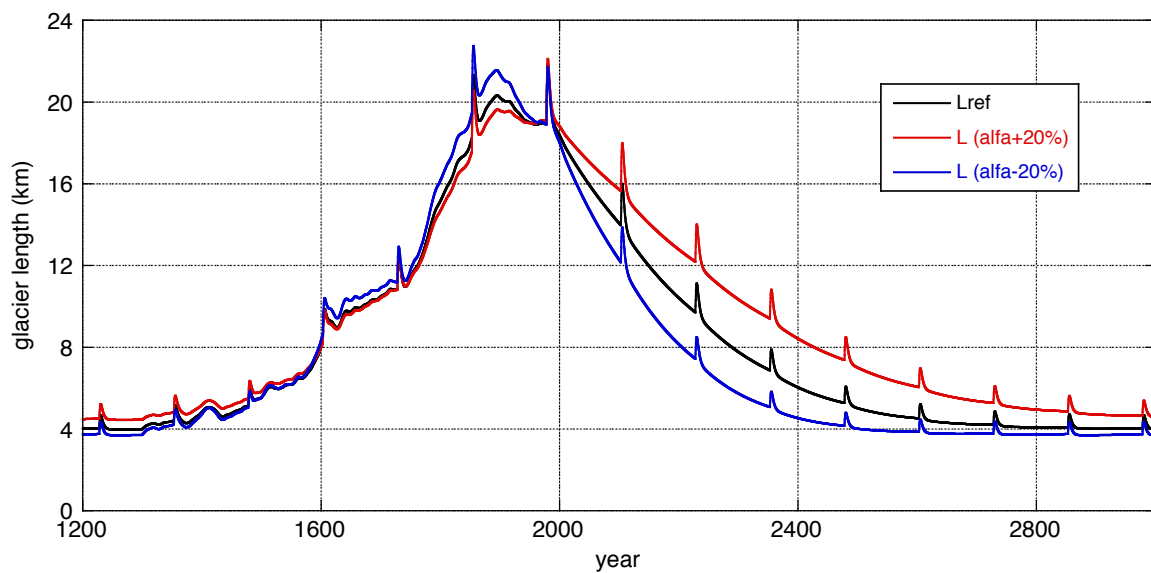
15

16



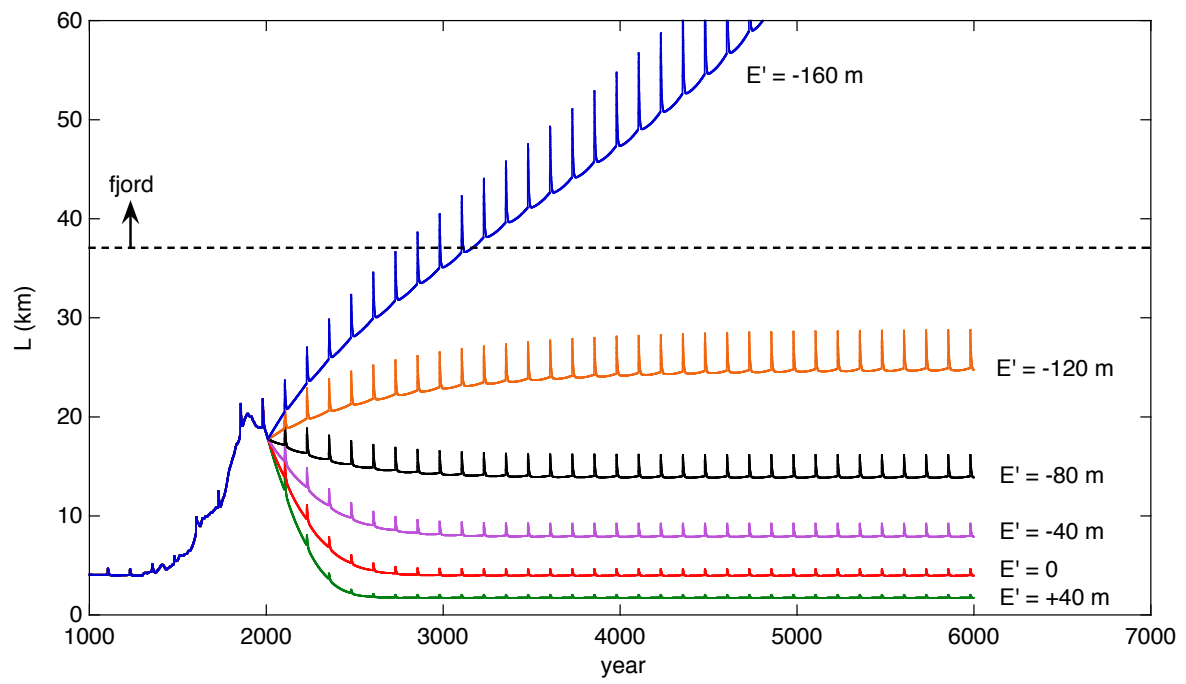
1
2
3
4
5
6
7
8
9
10
11
12
13
14
15
16
17
18
19

Fig. 10. The effect of surges on the evolution of Abrahamsenbreen. The ‘reference’ simulation is the same as in Fig. 8 (note that this simulation has a 125 yr surging period).



1
2
3
4
5
6
7
8
9
10
11
12
13
14
15
16
17
18
19

Fig. 11. The effect of different values of α_m on the simulated glacier length. The ‘reference’ simulation is shown in read.



1

2 **Fig. 12.** Simulated evolution of Abrahamsenbreen for some selected values of the equilibrium-
 3 line altitude (relative to the mean value for the period 1989-2010).

4

5

6

7

8

9

10

11

12

13

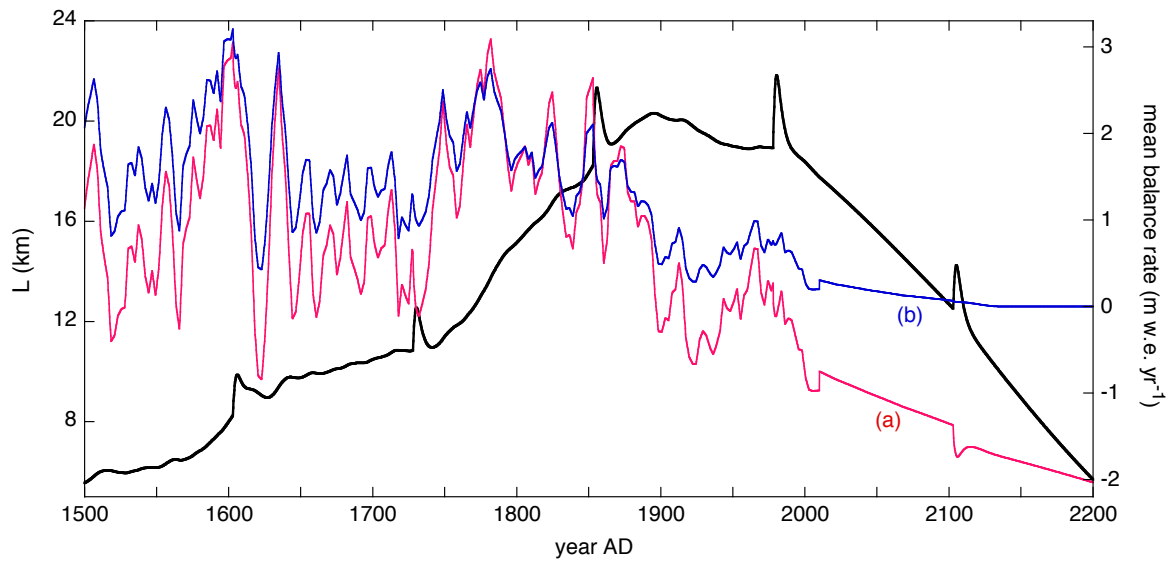
14

15

16

17

18



1

2 **Fig. 13.** Simulated evolution of Abrahamsenbreen in the case of a rise of the equilibrium line
 3 of 1 m yr^{-1} . Glacier length in black (scale at left). The curve labeled (a) shows the net balance
 4 over the entire glacier system; the curve labelled (b) given the mass input from the tributary
 5 glaciers, expressed as a mean balance rate.

6

7